Supporting Information

Electronically Excited OH Super Rotors from Water Photodissociation by Using Vacuum Ultraviolet Free-Electron Laser Pulses

Yao Chang[1#], Feng An[2#], Qinming Li[1,5#], Zijie Luo[1,3], Li Che[3], Jiayue Yang[1], Zhichao Chen[1], Weiqing Zhang[1], Guorong Wu[1], Xixi Hu[2*], Daiqian Xie[2], Kaijun Yuan[1,5*], Xueming Yang[1,4]

1. *State key Laboratory of Molecular Reaction Dynamics, Dalian Institute of Chemical Physics, Chinese Academy of Sciences, 457 Zhongshan Road, Dalian, 116023, China*
2. *Key Laboratory of Mesoscopic Chemistry, School of Chemistry and Chemical Engineering, Institute of Theoretical and Computational Chemistry, Nanjing University, Nanjing 210093, China*
3. *Department of Physics, School of Science, Dalian Maritime University, 1 Linghai Road, Dalian, Liaoning 116026, P. R. China*
4. *Department of Chemistry, Southern University of Science and Technology, Shenzhen 518055, China*
5. *University of Chinese Academy of Sciences, Beijing 100049, P. R. China*

1. Dissociation Channels at 96.4 nm Photolysis

The initial excitation of H_2O at 96.4 nm in this work is to a high-lying Rydberg state. Since the first ionization potential of H_2O is 12.6 eV (98.2 nm), the vertical excitation energy of this Rydberg state has already above the ionization limit. With the references, the ionization quantum yield of H_2O at this wavelength is ~0.3[1,2], which means about 70% of H_2O molecules still remain neutral (which is called super excited states). The photofragmentation of such super excited molecules is important in the upper ionosphere of the planets and in the photodissociation region of the planetary nebula. Possible dissociation channels for H_2O following excitation at 96.4 nm are listed below, along with the corresponding thermo-chemical threshold energy[3]

$$H_2O + h\nu \rightarrow H + OH\ (X^2\Pi) \qquad E_T \leqslant 62{,}580\ cm^{-1}$$

$$H + OH\ (A^2\Sigma^+) \qquad E_T \leqslant 30{,}141\ cm^{-1}$$

$$H + O\ (^3P) + H \qquad E_T \leqslant 27{,}157\ cm^{-1}$$

$$H + O\ (^1D) + H \qquad E_T \leqslant 11{,}291\ cm^{-1}$$

The total translational energy (E_T) spectra have been recorded previously with the wavelength between 121-132 nm[4,5]. Comparing with those results, the sharp structures were dominant, and the broad component underlying those structures was only observed at the excitation energies above the threshold of triple dissociation channel O (^{3}P) + 2H, which suggests the broad component arises from the triple dissociation channel, and the extensive sharp structures are attributed to the rovibrational states of OH(A/X) fragments. This assumption can help us to fit the dissociation channels shown in Figure S1.

According to the above assumption, the broad structureless components are assigned to the triple dissociation channels, and the sharp structures are attributed to the binary dissociation channels. Then we use a Gaussian profile to simulate the population of each quantum state. The width of the profile for each quantum state used in the simulation varies according to the relative kinetic energy resolution ($\delta E/E$ <1%) and the FEL beam width. The intensities of each OH quantum state and of the broad feature (attributable to the triple fragmentation products) are adjusted to produce a summed simulated E_T spectrum that should match the experimental data. Recognizing that two H atoms are formed in the triple dissociation process, a branching ratio for the triple dissociation channels and the binary dissociation channels is ~0.8:0.2. We note that the branching fraction into the triple dissociation channels are least well determined, as this process has not been fully characterized in the experiment (The fitting error bar for the triple dissociation channel is estimated to be ± 10%). With the references, the absorption cross-section of H_2O at 96.4 nm is σ_{H2O}~1.7×10^{-17} cm^2, and the ionization fraction of H_2O at this wavelength is ~0.3. Thus the cross section for H+OH(*X/A*) product formation following 96.4 nm photodissociation of H_2O can be estimated to be $1.7\times10^{-17}\times(1-0.3)\times0.2$=~$2.4(\pm1.0)\times10^{-18}$ cm^2. About 30% of the OH products formed at this wavelength are in rotational levels with energies above the OH(A) dissociation limit, suggesting that the cross section for forming OH(A) “super rotors” in the 96.4 nm photolysis of H_2O at is ~$(0.7\pm0.3)\times10^{-18}$ cm^2.

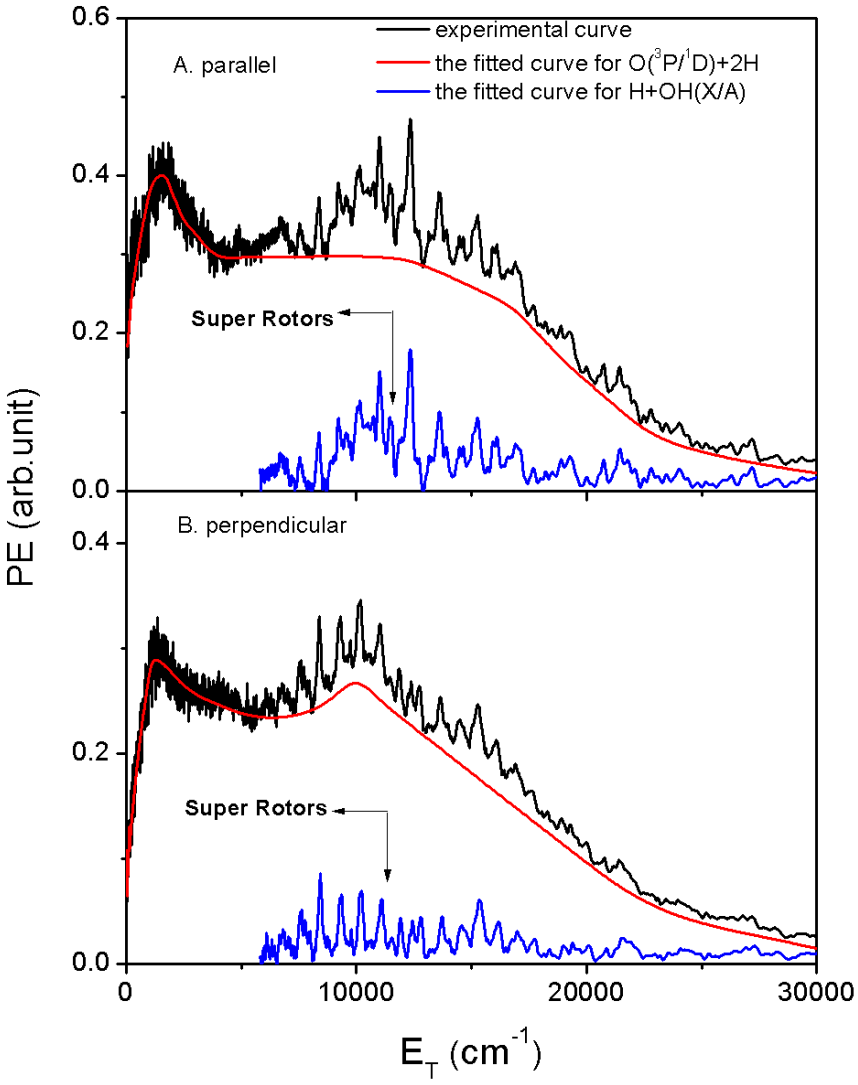

Figure S1 Deconvolutions of the E_T spectra derived from the H atom TOF spectra measured following 96.4 nm photolysis of H_2O into components associated with $O(^3P/^1D)+2H$ and H+OH(X/A) fragments.

Table S1 The E_T (OH (A, v'=0 and 1, j)) values for assignment shown in Figure 2.

	E_T (OH (A, v'=0, j)) $=h\nu$-D_0(H-OH)-$T_{v'=0,j}$ / cm^{-1}	E_T (OH (A, v'=1, j)) $=h\nu$-D_0(H-OH)-$T_{v'=1,j}$ / cm^{-1}
0	30141	27154
1	30107	27122
2	30039	27057
3	29937	26961
4	29802	26832
5	29633	26672
6	29431	26480
7	29196	26257
8	28929	26003
9	28630	25718
10	28298	25404
11	27936	25060
12	27543	24686
13	27120	24285
14	26667	23855
15	26185	23398
16	25675	22915
17	25138	22406
18	24574	21872
19	23984	21314
20	23369	20732
21	22730	20129
22	22068	19504
23	21384	18858
24	20679	18194
25	19954	17511
26	19210	16812
27	18449	16097
28	17671	15367
29	16878	14624
30	16071	13869
31	15252	13104
32	14421	12330
33	13581	11549
34	12733	10761
35	11878	9969
36	11019	9174
37	10155	8379
38	9290	7583

39	8425	6791
40	7562	6002
41	6702	5219
42	5848	4445
43	5003	

*The Term values of $T_{v',j}$ with j<33 are adapted from Ref. 34 in the main text, and the levels with j⩾33 are obtained by polynomial fitting. In a jet-cooled molecular beam, the rotational temperature of parent H_2O is quite cold, giving the $E_{int}(H_2O)$=~0.

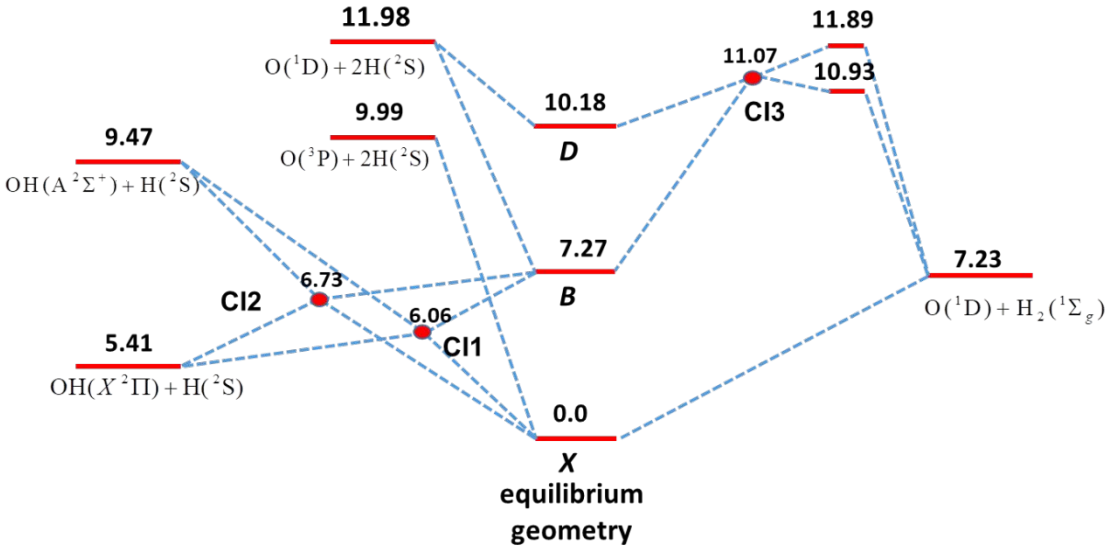

Figure S2. Energy level diagram for the binary and three-body dissociation of H_2O. The numbers are energies including zero-point energy with respect to the ground state energy (The unit is eV). There are two conical intersections (CIs) between the $\tilde{B}$ and $\tilde{X}$ states, which arise because for a linear approach of H to OH a repulsive potential curve from H+OH(X) can cross an attractive potential curve from H+OH(A), whereas there is an avoided crossing of these curves in the lower symmetry of a bent geometry.

2. Computational Details

The adiabatic potential energy curves (PECs) of the ground and six low-lying excited states of the OH radical have been calculated using the multi-reference configuration interaction (MRCI) method with the large basis set of aug-cc-pV5Z. The OH radical total 9 electrons that occupied in 6 orbitals while 1s orbital of the atom O is doubly occupied and not optimized in all configuration. The active space used here is [3110] for $[a_1b_1b_2a_2]$ using C_{2v} symmetry. The spin-orbit (SO) coupling matrix elements are considered in this work and computed by using the Breit–Pauli Hamiltonian at the same level. The PECs were constructed with the cubic spline interpolation method.

The dissociation energy, excitation energy and equilibrium bond length are in good agreement with the experimental values, as shown in Table S2. The SO Hamiltonian in the six-state diabatic basis is shown in Table S3.

Table S2. The dissociation energy, excitation energy and equilibrium bond length for the two electronic states.

		D_e / cm^{-1}	T_e / cm^{-1}	r_e / bohr
$X^2\Pi$	This work	37231.9	-	1.8289
	Expt.	37290	-	1.8325
$A^2\Sigma^+$	This work	20490.5	32573	1.9086
	Expt.	20476	32684.1	1.9126

Table S3. The SO Hamiltonian in the six-state diabatic basis.

$\hat{H}_{so}$	$\left\|X^2\Pi_+\right\rangle\left\|-\frac{1}{2}\right\rangle$	$\left\|^4\Pi_+\right\rangle\left\|-\frac{1}{2}\right\rangle$	$\left\|^4\Pi_-\right\rangle\left\|+\frac{3}{2}\right\rangle$	$\left\|A^2\Sigma^+\right\rangle\left\|+\frac{1}{2}\right\rangle$	$\left\|^2\Sigma^-\right\rangle\left\|+\frac{1}{2}\right\rangle$	$\left\|^4\Sigma^-\right\rangle\left\|+\frac{1}{2}\right\rangle$
$\left\|X^2\Pi_+\right\rangle\left\|-\frac{1}{2}\right\rangle$	A1	B1	0	B2	B3	B4
$\left\|^4\Pi_+\right\rangle\left\|-\frac{1}{2}\right\rangle$	B1	A2	0	B5	B6	B7
$\left\|^4\Pi_-\right\rangle\left\|+\frac{3}{2}\right\rangle$	0	0	A3	B8	B9	B10
$\left\|A^2\Sigma^+\right\rangle\left\|+\frac{1}{2}\right\rangle$	B2	B5	B8	0	B11	B12
$\left\|^2\Sigma^-\right\rangle\left\|+\frac{1}{2}\right\rangle$	B3	B6	B9	B11	0	0
$\left\|^4\Sigma^-\right\rangle\left\|+\frac{1}{2}\right\rangle$	B4	B7	B10	B12	0	0

References:

(1) Lee, L. C.; Suto, M. quantitative photoabsorption and fluorescence study of H_2O and D_2O at 50-190nm. *Chem. Phys.* **1986,** *110*, 161-169.

(2) Fillion, J. H.; Dulieu, F.; Baouche, S.; Lemaire, J. L.; Jochims, H. W.; Leach, S. Ionization yield and absorption spectra reveal superexcited Rydberg state relaxation processes in H_2O and D_2O. *J. Phys. B: At., Mol. Opt. Phys.* **2003,** *36*, 2767-2776.

(3) Harich, S. A.; Hwang, D. W. H.; Yang, X.; Lin, J. J.; Yang, X.; Dixon, R. N. Photodissociation of H_2O at 121.6 nm: A state-to-state dynamical picture. *J. Chem. Phys.* **2000,** *113*, 10073-10090.

(4) K. J. Yuan; R. N. Dixon; Yang, X. M. Photochemistry of the Water Molecule: Adiabatic versus Nonadiabatic Dynamics. *Acc. Chem. Res.* **2011,** *44*, 369-378.

(5) K. Yuan; Y. Cheng; L. Cheng; Q. Guo; D. Dai; X. Wang; X. Yang; Dixon, R. N. Nonadiabatic dissociation dynamics in H_2O: Competition between rotationally and nonrotationally mediated pathways. *Proc. Natl. Acad. Sci. U S A* **2008,** *105* 19148–19153.